

See discussions, stats, and author profiles for this publication at: <https://www.researchgate.net/publication/257836154>

Catalytic Partial Oxidation of Methane over Perovskite La₄Sr₈Ti₁₂O₃₈-delta Solid Oxide Fuel Cell (SOFC) Anode Material in an Oxygen-Permeable Membrane Reactor

ARTICLE *in* ENERGY & FUELS · FEBRUARY 2010

Impact Factor: 2.79 · DOI: 10.1021/ef900995t

CITATIONS

16

READS

82

4 AUTHORS, INCLUDING:



[Wendong Wang](#)

University of Science and Technology of China

39 PUBLICATIONS 1,069 CITATIONS

[SEE PROFILE](#)

Catalytic Partial Oxidation of Methane over Perovskite $\text{La}_4\text{Sr}_8\text{Ti}_{12}\text{O}_{38-\delta}$ Solid Oxide Fuel Cell (SOFC) Anode Material in an Oxygen-Permeable Membrane Reactor

Min-Chuan Zhan,[†] Wen-Dong Wang,^{*,†,‡} Ting-Fang Tian,[†] and Chu-Sheng Chen[†]

[†]CAS Key Laboratory of Materials for Energy Conversion, Department of Materials Science and Engineering and

[‡]Department of Chemical Physics, University of Science and Technology of China, Hefei 230026, China

Received September 8, 2009. Revised Manuscript Received October 21, 2009

The partial oxidation of methane to syngas over perovskite $\text{La}_4\text{Sr}_8\text{Ti}_{12}\text{O}_{38-\delta}$ solid oxide fuel cell (SOFC) anode material was studied with a $\text{Ce}_{0.8}\text{Sm}_{0.2}\text{O}_{2-\delta}-\text{La}_{0.8}\text{Sr}_{0.2}\text{CrO}_{3-\delta}$ dual-phase composite membrane reactor. The catalytic activity strongly depends upon both the reaction temperature and CH_4 feed rate or O_2/CH_4 ratio. Approximately 88% CO and 89% H_2 selectivity at 30% CH_4 conversion can be achieved under the optimized membrane reactor operating conditions at 950 °C and CH_4 feed rate of 20 mL min^{-1} . Under more severe conditions at a higher CH_4 feed rate, $\text{La}_4\text{Sr}_8\text{Ti}_{12}\text{O}_{38-\delta}$ in the membrane reactor exhibits favorable stability and a facile catalyst regeneration process against carbon deposition. The reaction mechanism is explored by a comparative study with a conventional fixed-bed reactor, suggesting a direct CH_4 partial oxidation route below 800 °C and obvious CO_2 and steam reforming activities above 850 °C. The reaction pathway would involve lattice oxygen species and a surface formaldehyde intermediate, which could explain the difference in the reactivity for both reactors. The possible application of this reaction in the membrane reactor was discussed with respect to the syngas production and characterization on the catalytic behavior of SOFC anode material for the direct methane fuel cell by simulating a SOFC anode operating environment.

1. Introduction

Partial oxidation of methane (POM) has attracted rising attention as an alternative route to steam reforming for the production of syngas ($\text{CO} + \text{H}_2$).¹ During this process, the use of natural gas can be realized by converting methane to syngas with a ratio of H_2/CO equal to 2, which is a suitable feedstock for the synthesis of hydrocarbons or methanol, and the subsequent production of liquid fuels via existing processes, such as a Fischer–Tropsch reaction.² However, the established industrial process of noncatalytic partial oxidation of methane to syngas requires the severe operation conditions of very high temperature and high pressure.³ In the case of catalytic partial oxidation of methane conducted with a conventional co-fed reactor, the main disadvantage lies in the consumption of large quantities of pure oxygen that is produced by cryogenic separation from air with significant cost.⁴

A recent development in syngas production technology is performed with an oxygen-permeable dense ceramic mem-

brane reactor.^{4–10} This development combines the oxygen separation and POM process into a single step, which may eliminate the capital cost of oxygen production and avoid the safety problems aroused by premixing oxygen and methane in the co-fed reactor. The operating conditions of POM in the membrane reactor impose stringent requirements on the stability and oxygen permeability of the membrane¹¹ as well as the performance of catalysts for the POM reaction. The key to success in the membrane-based syngas production is to explore membrane materials possessing both high oxygen flux and long-term stability under the operating conditions.⁵ Our previous research^{12,13} has demonstrated that a $\text{Ce}_{0.8}\text{Sm}_{0.2}\text{O}_{2-\delta}-\text{La}_{0.8}\text{Sr}_{0.2}\text{CrO}_{3-\delta}$ dual-phase composite membrane may exhibit considerable oxygen permeability at elevated temperatures and satisfy the stability requirement under a large oxygen gradient, with one side exposed to air and the other side exposed to CO , CH_4 , or H_2 .

With respect to the catalysts for the POM reaction, metal catalysts based on nickel, cobalt, and noble metal have been demonstrated as the most active and selective ones.^{1,5,6,14–17} Additionally, recent investigations have demonstrated that some oxide catalysts exhibit interesting activity for POM under various reaction conditions, such as yttrium-stabilized

*To whom correspondence should be addressed. Telephone: +86-551-3603683. Fax: +86-551-3601592. E-mail: wangwd@ustc.edu.cn.

(1) York, A. P. E.; Xiao, T. C.; Green, M. L. H. *Top. Catal.* **2003**, *22*, 345–358.

(2) Freide, J.; Gamlan, T. D.; Graham, C.; Hensman, J. R.; Nay, B.; Sharp, C. *Top. Catal.* **2003**, *26*, 3–12.

(3) Fox, J. M. *Catal. Rev.–Sci. Eng.* **1993**, *35*, 169–212.

(4) Balachandran, U.; Dusek, J. T.; Maiya, P. S.; Ma, B.; Mieville, R. L.; Kleefisch, M. S.; Udovich, C. A. *Catal. Today* **1997**, *36*, 265–272.

(5) Bouwmeester, H. J. M. *Catal. Today* **2003**, *82*, 141–150.

(6) Ishihara, T.; Takita, Y. *Catal. Surv. Jpn.* **2000**, *4*, 125–133.

(7) Chen, C. S.; Feng, S. J.; Ran, S.; Zhu, D. C.; Liu, W.; Bouwmeester, H. J. M. *Angew. Chem., Int. Ed.* **2003**, *42*, 5196–5198.

(8) Zhu, D. C.; Xu, X. Y.; Feng, S. J.; Liu, W.; Chen, C. S. *Catal. Today* **2003**, *82*, 151–156.

(9) Yang, W. S.; Wang, H. H.; Zhu, X. F.; Lin, L. W. *Top. Catal.* **2005**, *35*, 155–167.

(10) Hamakawa, S.; Sato, K.; Inoue, T.; Nishioka, M.; Kobayashi, K.; Mizukami, F. *Catal. Today* **2006**, *117*, 297–303.

(11) Fraude, J. R.; Kharton, V. V.; Yaremchenko, A.; Naumovich, E. *J. Power Sources* **2004**, *130*, 77–84.

(12) Yi, J. X.; Zuo, Y. B.; Liu, W.; Winnubst, L.; Chen, C. S. *J. Membr. Sci.* **2006**, *280*, 849–855.

(13) Wang, B.; Yi, J. X.; Winnubst, L.; Chen, C. S. *J. Membr. Sci.* **2006**, *286*, 22–25.

(14) Enger, B. C.; Lodeng, R.; Holmen, A. *Appl. Catal., A* **2008**, *346*, 1–27.

(15) Dissanayake, D.; Rosynek, M. P.; Kharas, K. C. C.; Lunsford, J. H. *J. Catal.* **1991**, *132*, 117–127.

(16) Ashcroft, A. T.; Cheetham, A. K.; Foord, J. S.; Green, M. L. H.; Grey, C. P.; Murrell, A. J.; Vernon, P. D. F. *Nature* **1990**, *344*, 319–321.

(17) Hickman, D. A.; Schmidt, L. D. *Science* **1993**, *259*, 343–346.

zirconia (YSZ),^{18,19} Gd- and Nb-doped ceria,^{20,21} and La-FeO₃ and La_{1-x}Sr_xMnO₃-based perovskite oxides.^{22,23} However, the POM activity of these oxide catalysts is not as high as that of metal catalysts, which may hardly enable their direct application for the production of syngas.

Nickel-based catalysts have been extensively employed for the methane conversion in the membrane reactor.^{5–8,10,24–27} Although nickel is highly active for syngas production, it also catalyzes the formation of carbon from hydrocarbons under reducing conditions. The rapid deactivation of Ni-based catalysts for POM is mainly due to the serious carbon deposition, metal sintering, and loss of nickel during the high flow rate under the reaction conditions.¹⁴

The similar disadvantage of carbon deposition at nickel cermet anode also occurs for the direct oxidation of methane in a solid oxide fuel cell (SOFC) system.²⁸ One approach toward overcoming this limitation of Ni-based materials has focused on the development of alternative materials,^{28,29} for example, perovskite-type transition-metal oxides, which are catalytically active for the oxidation of methane. The modified perovskite-structured La₄Sr₈Ti₁₂O_{38-δ} oxides have been investigated as promising anode material, which are considerably active for the direct oxidation of CH₄ at high temperature in the SOFC system.^{30,31} The catalytic properties of anode materials are very important in determining the overall SOFC performance. Therefore, there is evidently a need for fundamental studies on the mechanisms of the catalytic reactions occurring on the anode. However, the essential insight into the catalytic reaction is rather limited because of the complexity of reaction mechanisms and the limitation of experimental techniques with respect to an operating SOFC anode.

In the present work, the oxidation of methane over perovskite La₄Sr₈Ti₁₂O_{38-δ} catalyst was investigated in an oxygen-permeable membrane reactor constructed using a Ce_{0.8}Sm_{0.2}O_{2-δ}–La_{0.8}Sr_{0.2}CrO_{3-δ} composite membrane tube. Appreciable catalytic activity toward the POM reaction was observed for the first time over this SOFC anode material in the membrane reactor, as well as the favorable stability and facile catalyst regeneration process against carbon deposition. The reaction mechanisms were discussed on the basis of the comparative studies in the conventional fixed-bed reactor.

- (18) Steghuis, A. G.; van Ommen, J. G.; Lercher, J. A. *Catal. Today* **1998**, *46*, 91–97.
- (19) Zhu, J. J.; van Ommen, J. G.; Lefferts, L. J. *J. Catal.* **2004**, *225*, 388–397.
- (20) Ramirez-Cabrera, E.; Atkinson, A.; Chadwick, D. *Appl. Catal., B* **2002**, *36*, 193–206.
- (21) Ramirez-Cabrera, E.; Laosiripojana, N.; Atkinson, A.; Chadwick, D. *Catal. Today* **2003**, *78*, 433–438.
- (22) Dai, X. P.; Li, R. J.; Yu, C. C.; Hao, Z. P. *J. Phys. Chem. B* **2006**, *110*, 22525–22531.
- (23) Wei, H. J.; Cao, Y.; Ji, W. J.; Au, C. T. *Catal. Commun.* **2008**, *9*, 2509–2514.
- (24) Feng, S. J.; Ran, S.; Zhu, D. C.; Liu, W.; Chen, C. S. *Energy Fuels* **2004**, *18*, 385–389.
- (25) Jiang, H. Q.; Wang, H. H.; Werth, S.; Schiestel, T.; Caro, J. *Angew. Chem., Int. Ed.* **2008**, *47*, 9341–9344.
- (26) Zhu, X. F.; Li, Q. M.; Cong, Y.; Yang, W. S. *Catal. Commun.* **2008**, *10*, 309–312.
- (27) Kondratenko, E. V.; Wang, H. H.; Kondratenko, V. A.; Caro, J. *J. Mol. Catal. A: Chem.* **2009**, *297*, 142–149.
- (28) Atkinson, A.; Barnett, S.; Gorte, R. J.; Irvine, J. T. S.; McEvoy, A. J.; Mogensen, M.; Singhal, S. C.; Vohs, J. *Nat. Mater.* **2004**, *3*, 17–27.
- (29) Sun, C. W.; Stimming, U. *J. Power Sources* **2007**, *171*, 247–260.
- (30) Ruiz-Morales, J. C.; Canales-Vazquez, J.; Savaniu, C.; Marrero-Lopez, D.; Zhou, W. Z.; Irvine, J. T. S. *Nature* **2006**, *439*, 568–571.
- (31) Canales-Vazquez, J.; Tao, S. W.; Irvine, J. T. S. *Solid State Ionics* **2003**, *159*, 159–165.

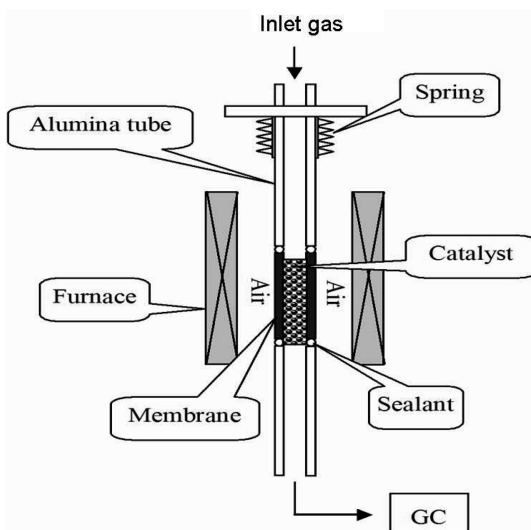


Figure 1. Schematic of the SDC–LSC membrane reactor.

2. Experimental Section

2.1. Sample Preparation and Characterization. Fluorite Ce_{0.8}Sm_{0.2}O_{2-δ} (SDC) powder was prepared by an oxalate complexation precipitation route starting from Ce(NO₃)₃·6H₂O (> 99%) and Sm₂O₃ (> 99.99%). Perovskite La_{0.8}Sr_{0.2}CrO_{3-δ} (LSC) powder was synthesized using a conventional solid-state reaction route from SrCO₃ (> 99%), La₂O₃ (> 99.99%), and Cr₂O₃ (> 99%), as described in detail elsewhere.¹²

The membrane was prepared using a standard ceramic method. The obtained SDC and LSC powders were thoroughly mixed by ball milling at a volume ratio of 60:40 (weight ratio of 63:37). The mixture was then isostatically pressed into a tube under a pressure of 300 MPa and finally sintered at 1550 °C for 10 h.

The La₄Sr₈Ti₁₂O_{38-δ} catalyst was prepared by a modified Pechini method. Tetraethyl titanate (> 98.0%) was dissolved in ethylene glycol and citric acid to form a stable solution, which can be mixed with the appropriate Sr and La nitrate aqueous solutions without causing any precipitation. The molar ratio of citric acid to Ti was 2, while that of acid to Sr and La was 0.5 in the solution. The final clear solution was evaporated at 80 °C until a gel was formed, which was then kept in an oven at 250 °C overnight to obtain brown powder. The resulting powder was treated at 600 °C for 4 h to burn out the organic substance and then calcined at 1000 °C for 6 h to form the expected crystalline phase. The final white powder was pressed into granular catalyst at a range of 0.25–0.5 mm for the following catalytic reaction tests. The Ni/γ-Al₂O₃ catalyst was prepared by an impregnation method, as described in the previous work.²⁴

The phase composition was analyzed by powder X-ray diffraction (XRD) performed with a Philips X'Pert Pro Super diffractometer (Cu Kα = 0.15406 nm). The microstructure of the samples was examined with scanning electron microscopy (SEM) using a JEOLJSM-6700F instrument. The Brunauer–Emmett–Teller (BET) surface area was determined from a N₂ adsorption–desorption isotherm measured with a Coulter 3100 system.

2.2. Membrane Reactor Setup. Figure 1 indicates a schematic of the membrane reactor used in the present study. The outer wall of the sintered membrane tube was polished and ultrasoonically cleaned in ethanol prior to usage. The membrane reactor was constructed by sealing the SDC–LSC membrane tube between two alumina tubes with glass rings as a sealant at elevated temperature up to 1020 °C in stagnant air. The catalysts or quartz particles were packed in the membrane tube supported by quartz wool. Under the operating conditions, the outer wall of the membrane tube was exposed to the ambient air, while the

Table 1. Summary of CH₄ Oxidation over Different Catalysts in the SDC–LSC Membrane Reactor^a

catalyst	CH ₄ conversion (%)	selectivity (%)					P_{syn} (mL cm ⁻² min ⁻¹)
		CO ₂	CO	H ₂	C ₂ H _x	$\sum C$ (mmol h ⁻¹)	
La ₄ Sr ₈ Ti ₁₂ O _{38-δ} ^b	30.1	12.1	87.8	88.8	0.1	48.1	2.45
La ₄ Sr ₈ Ti ₁₂ O _{38-δ}	18.1	27.1	72.7	69.7	0.2	47.3	0.08
quartz	9.8	86.5	5.9	14.6	7.7	51.1	7.29
Ni catalyst	84.1	0.2	99.8	100	0.0		

^a Operation conditions: reaction temperature at 950 °C and CH₄ feed rate at 20 mL min⁻¹. ^b CH₄ oxidation in the fixed-bed reactor at 950 °C and O₂/CH₄ ratio equal to 0.2.

inlet gas methane was fed into the reactor from the top at various flow rates to react with the oxygen permeated from the air side.

2.3. CH₄ Oxidation Reaction. The oxidation of methane in the membrane reactor was investigated at the temperature ranging from 800 to 950 °C and at the inlet CH₄ flow rate varying from 10 to 40 mL min⁻¹. Typically, a membrane tube of 29.0 mm in length, 6.86 mm in inner diameter, and 0.72 mm in wall thickness was packed with 1.07 mL of the catalyst inside. The reaction temperature was controlled within 0.2 °C at the set point (Yudian AI-708P) and measured with another thermocouple attached to the membrane tube. The flow rate of inlet gas was regulated with a mass flow controller (Sevenstar D07-12A/ZM). The gas composition in the effluent was analyzed by two gas chromatographs. Shimadzu GC-14C with a 5A molecular sieve column was used for the separation of H₂, O₂, N₂, CH₄, and CO, while Fuli GC-9750 with a GDX-502 column was used for CO₂ and C₂ hydrocarbons (C₂H_x). Concentrations of the monitored gas components were calculated by calibration with reference to a standard gas mixture in the known quantities. The amount of H₂O was determined on the basis of the hydrogen atomic balance. The oxygen permeation flux was calculated on the basis of the oxygen atomic balance of all of the products containing oxygen. The conversion of CH₄ (X_{CH_4}) and selectivity to CO (S_{CO}) and H₂ (S_{H_2}) were defined as follows:

$$X_{\text{CH}_4} = \frac{F_{\text{CH}_4}^{\text{in}} - F_{\text{CH}_4}^{\text{out}}}{F_{\text{CH}_4}^{\text{in}}}; \quad S_{\text{CO}} = \frac{F_{\text{CO}}^{\text{out}}}{F_{\text{CO}}^{\text{out}} + F_{\text{CO}_2}^{\text{out}} + F_{\text{C}_2\text{H}_x}^{\text{out}}};$$

$$S_{\text{H}_2} = \frac{F_{\text{H}_2}^{\text{out}}}{2(F_{\text{CO}}^{\text{out}} + F_{\text{CO}_2}^{\text{out}} + 2F_{\text{C}_2\text{H}_x}^{\text{out}})}$$

For the comparison purpose, the catalytic conversion of methane was also carried out with a conventional fixed-bed reactor. The catalyst (500 mg) was loaded into a vertical tubular quartz reactor (8 mm inner diameter) and kept in the isothermal center part of the reactor supported using a flock of quartz wool. The total flow rate was maintained at 100 mL min⁻¹ balanced with nitrogen, and the flow rate of CH₄ was fixed at 10 mL min⁻¹. For the oxidation of methane, various ratios of oxygen to methane were adjusted to simulate different atmospheres. In addition, CO₂ and H₂O reforming of methane were also examined under the given conditions. The steam was added to the reaction by passing the reactant mixture through a steam saturator, and the partial pressure of steam was determined by the temperature of the saturator. The activity measurements were performed under static isothermal conditions, with the reaction temperature up to 950 °C. After the stabilization at each temperature for 30 min, the reactants and products were analyzed by the gas chromatographs. Repetition tests were conducted to ensure the reproducibility. Conversion (X) and yields (Y) were calculated according to

$$X_{\text{O}_2} = \frac{F_{\text{O}_2}^{\text{in}} - F_{\text{O}_2}^{\text{out}}}{F_{\text{O}_2}^{\text{in}}}; \quad Y_{\text{CO}} = \frac{F_{\text{CO}}^{\text{out}}}{F_{\text{CH}_4}^{\text{in}}};$$

$$Y_{\text{H}_2} = \frac{F_{\text{H}_2}^{\text{out}}}{2F_{\text{CH}_4}^{\text{in}}}; \quad Y_{\text{CO}_2} = \frac{F_{\text{CO}_2}^{\text{out}}}{F_{\text{CH}_4}^{\text{in}}}$$

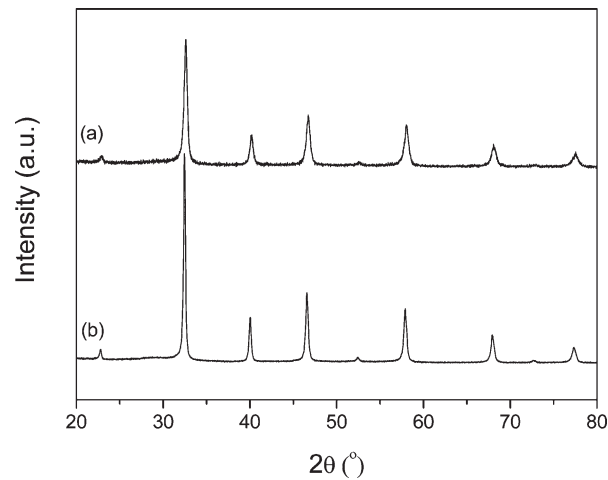


Figure 2. XRD patterns of (a) fresh La₄Sr₈Ti₁₂O_{38-δ} catalyst and (b) La₄Sr₈Ti₁₂O_{38-δ} catalyst used in the membrane reactor for about 600 h.

3. Results

3.1. Samples Characterization. The BET surface areas determined from a N₂ adsorption–desorption isotherm for La₄Sr₈Ti₁₂O_{38-δ} is 8.2 m² g⁻¹. Figure 2 indicates the XRD patterns of the catalyst before and after the methane oxidation reaction. The fresh catalyst can be assigned to a single cubic perovskite-type structure. After the reaction in the membrane reactor for hundreds of hours, La₄Sr₈Ti₁₂O_{38-δ} may retain its phase composition without the observation of any extra peak. It is noticed that all diffraction peaks of the perovskite phase become sharper and shift slightly to a lower angle after reaction, which may relate to the agglomeration of catalyst particles and the increase in the cell parameter from 0.3889(8) to 0.3900(9) nm after the long-term reaction. The increase in the cell parameter may result from a decrease in lattice oxygen stoichiometry in the perovskite structure during the prolonged reaction under a reducing atmosphere.³²

3.2. Oxidation of CH₄ in the SDC–LSC Membrane Reactor. The catalytic performances of CH₄ oxidation over different catalysts in the SDC–LSC membrane reactor are compared in Table 1 under the representative operation conditions of the reaction temperature at 950 °C and CH₄ feed rate at 20 mL min⁻¹. The coincidence of the total carbon ($\sum C$) balance under the identical operation conditions ensures the reliability of the product analysis processes in all of the cases. In fact, CH₄ may be converted with a conversion of 9.8% and mainly oxidized to CO₂ with a selectivity of 86.5% in the presence of the inert quartz packed inside the membrane tube. It is noticeable that the perovskite catalyst

(32) Marina, O. A.; Canfield, N. L.; Stevenson, J. W. *Solid State Ionics* 2002, 149, 21–28.

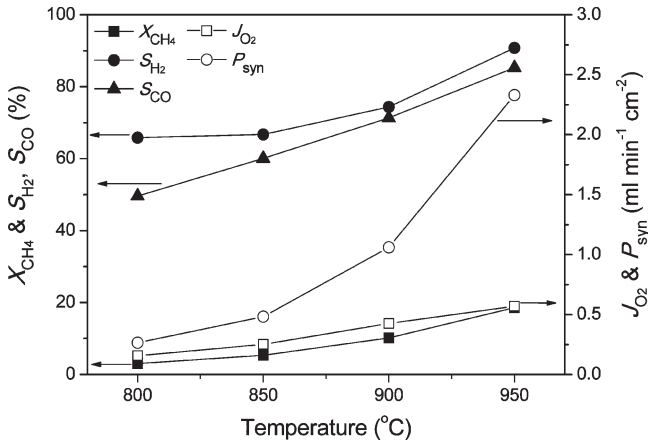


Figure 3. Influence of the reaction temperature on CH₄ oxidation in the SDC–LSC membrane reactor packed with the La₄Sr₈Ti₁₂O_{38-δ} catalyst at a CH₄ feed rate of 30 mL min⁻¹.

La₄Sr₈Ti₁₂O_{38-δ} exhibits appreciable catalytic activity toward the POM reaction, with H₂ and CO as the predominant products of CH₄ oxidation in the membrane reactor, although the CH₄ conversion, H₂ and CO selectivity, and syngas production rate (P_{syn}) are rather lower than those of the Ni-based catalyst.

Figure 3 presents the influence of the reaction temperature on the catalytic performance of CH₄ oxidation in the SDC–LSC membrane reactor packed with the La₄Sr₈Ti₁₂O_{38-δ} catalyst at a fixed CH₄ feed rate. The oxygen permeation rate (J_{O_2}) increases with temperature from 800 to 950 °C as expected, mainly because of the increasing oxygen ionic and electric conductivities of the dual-phase composite membrane, which was proven stable, and considerable oxygen permeability under air/He and air/CH₄ gradients in our previous studies.^{12,13} It is observed that the main products of CH₄ oxidation are H₂ and CO in the membrane reactor starting from 800 °C. With the reaction temperature elevated up to 950 °C, the conversion of CH₄ rises evidently from 3.0 to 18.6%, which is not only attributed to the apparently increased oxygen permeation rate from 0.16 to 0.57 mL cm⁻² min⁻¹ but also accompanied by the significantly enhanced selectivity to CO and H₂ from 49.6 and 65.8 to 85.3% and 90.8%, respectively. The enhancements of oxygen permeability and catalytic performance give rise to a remarkable promotion of the syngas production rate from 0.27 to 2.33 mL cm⁻² min⁻¹.

The influence of the CH₄ feed rate on the catalytic performance of CH₄ oxidation over the La₄Sr₈Ti₁₂O_{38-δ} catalyst in the SDC–LSC membrane reactor is shown in Figure 4 when the reactor is operated at the fixed temperature of 950 °C. It is observed that the methane conversion decreases from 51.5 to 13.7%, while the CH₄ feed rate increases from 10 to 40 mL min⁻¹, which is consistent with the fact that the total oxygen permeation rate remains relatively steady at the fixed temperature. In fact, the oxygen permeation rate J_{O_2} decreases slightly with the increasing CH₄ feed rate, which could be attributed to the carbon deposition at a higher CH₄ feed rate, as described later. However, the selectivity to CO and H₂ as well as the syngas production rate enhance apparently, while the CH₄ feed rate increases from 10 to 20 mL min⁻¹. With a CH₄ feed rate further increasing to 40 mL min⁻¹, the syngas production rate remains almost constant, while S_{CO} decreases and S_{H_2}

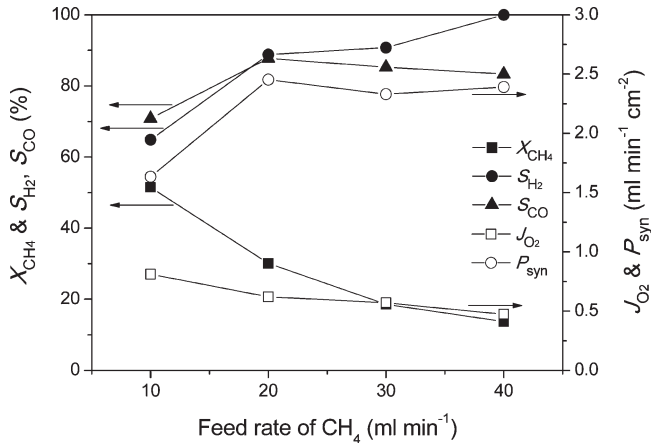


Figure 4. Influence of the CH₄ feed rate on CH₄ oxidation in the SDC–LSC membrane reactor packed with the La₄Sr₈Ti₁₂O_{38-δ} catalyst at 950 °C.

increases to some extent, respectively. It is noticed that the optimized syngas production rate as high as 2.45 mL cm⁻² min⁻¹ with the ideal ratio of H₂ to CO equal to 2.0 is achieved at the CH₄ feed rate of 20 mL min⁻¹ in the company of the almost identical selectivity S_{CO} (87.8%) and S_{H_2} (88.8%).

It was examined that the carbon deposition occurring for perovskite La₄Sr₈Ti₁₂O_{38-δ} was much less serious than that for the Ni-based catalyst after testing for 100 h in the membrane reactor under the optimized reaction conditions at 950 °C and the CH₄ feed rate of 20 mL min⁻¹. Thus, a long-term stability test was performed under more severe conditions at a higher CH₄ feed rate of 30 mL min⁻¹, as well as the regeneration process of the La₄Sr₈Ti₁₂O_{38-δ} catalyst. Figure 5 indicates the stability test for about 600 h on stream, including the regeneration process of three cycles.

Initially, it takes 25 h for the reaction system to reach the maximum of the POM reactivity, which features the highest P_{syn} of 2.27 mL cm⁻² min⁻¹ by achieving 88.1% H₂ and 84.2% CO selectivity at 18.5% CH₄ conversion. The time span of the stable operation state is more than 42 h, during which 90% of the highest P_{syn} value can be maintained. A subsequent deactivation occurs gradually, and the degraded catalytic performance leads to the deteriorative P_{syn} value as low as 0.88 mL cm⁻² min⁻¹ after 110 h on stream, which may be mainly due to the carbon deposition. The reaction system was then subjected to a recovering treatment by simply switching the inlet gas from CH₄ to air flow over 10 h under the reaction conditions to remove the carbon deposition, which was followed by switching back to CH₄ flow and starting the next running cycle.

The second cycle commences with a partially recovered P_{syn} of 1.61 mL cm⁻² min⁻¹, and the reaction system takes a rather extended activation stage of 106 h to attain its maximum P_{syn} of 2.24 mL cm⁻² min⁻¹ (84.2% H₂ and 82.0% CO selectivity at 18.4% CH₄ conversion). In comparison to the first cycle, the peak values are almost identical and an improved time span of the stable operation state is obtained at about 53 h. This cycle operates for 200 h on stream prior to the P_{syn} value decreasing to 0.73 mL cm⁻² min⁻¹ and then another recovering treatment. During the third cycle, although the maximum performance (P_{syn} of 1.66 mL cm⁻² min⁻¹ with 76.2% H₂ and 73.5% CO selectivity at 15.2% CH₄ conversion) is lower than those of both former cycles to some extent, the time span of the stable operation

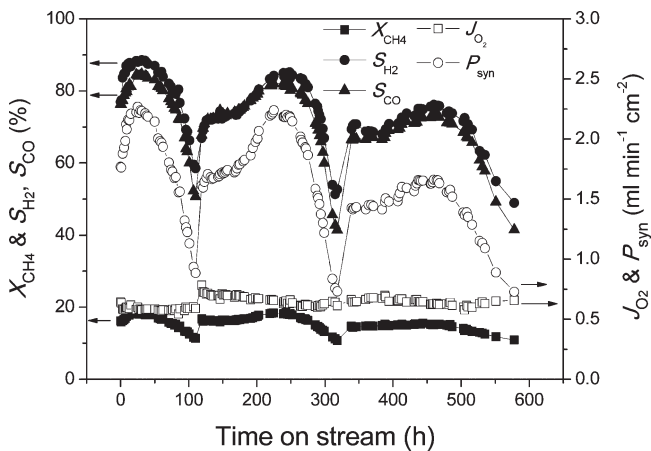


Figure 5. Stability test and regeneration process of the $\text{La}_4\text{Sr}_8\text{Ti}_{12}\text{O}_{38-\delta}$ catalyst for CH_4 oxidation in the SDC–LSC membrane reactor at 950°C and CH_4 feed rate of 30 mL min^{-1} .

state is prolonged to around 98 h. These results suggest that the POM reaction performance over the $\text{La}_4\text{Sr}_8\text{Ti}_{12}\text{O}_{38-\delta}$ catalyst in the SDC–LSC membrane reactor may decrease because of the escalating carbon deposition during each operating cycle, while the simple recovering treatment may be successful in regenerating the reaction system, and the time span of the stable operation state can be effectively increased.

The whole stability test under reaction conditions for about 600 h ended up with the deterioration of POM reactivity because of severe carbon deposition, which was revealed by the SEM images. As shown in Figure 6a, the $\text{La}_4\text{Sr}_8\text{Ti}_{12}\text{O}_{38-\delta}$ catalyst surface is mostly covered by amorphous graphitic carbon species.^{33–35} However, the phase composition of the perovskite catalyst remains stable, except that slight agglomeration occurs, as suggested from XRD results (Figure 1). With respect to the SDC–LSC membrane, only a small amount of spherical carbon sporadically deposits on the inner surface (Figure 6b), which is also in accordance with the observation that the total oxygen permeation rate J_{O_2} remains relatively steady during most of the time of the stability test process (Figure 5).

3.3. Oxidation and Reforming of CH_4 in a Fixed-Bed Reactor. For the purpose of comparison, the catalytic behavior of CH_4 oxidation in the presence of the $\text{La}_4\text{Sr}_8\text{Ti}_{12}\text{O}_{38-\delta}$ catalyst was also investigated in the conventional fixed-bed reactor under various conditions. Figure 7 shows conversions and yields for methane oxidation as a function of the reaction temperature under a representative POM reaction condition. The contribution of the gas-phase reaction can be excluded on the basis of the observation of negligible conversions in the absence of catalyst. The catalyst becomes active above 500°C , and the major oxidation products are CO , CO_2 , H_2 , and H_2O . Appreciable CO and H_2 yields can be observed prior to the complete oxygen conversion at 750°C . Methane conversion reaches 34.4% at this temperature and increases slightly with the temperature to 38.3% at 950°C . Selectivity to the major products varies with the reaction temperature. In contrast to the temperature range

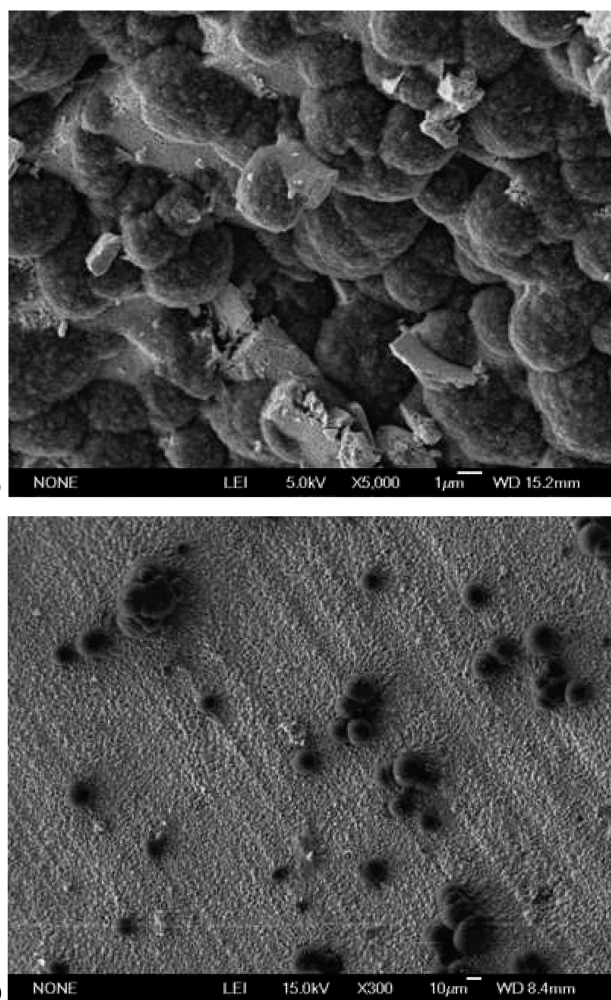


Figure 6. SEM images of the (a) $\text{La}_4\text{Sr}_8\text{Ti}_{12}\text{O}_{38-\delta}$ catalyst and (b) SDC–LSC membrane surface after the stability test and regeneration process under reaction conditions for 600 h.

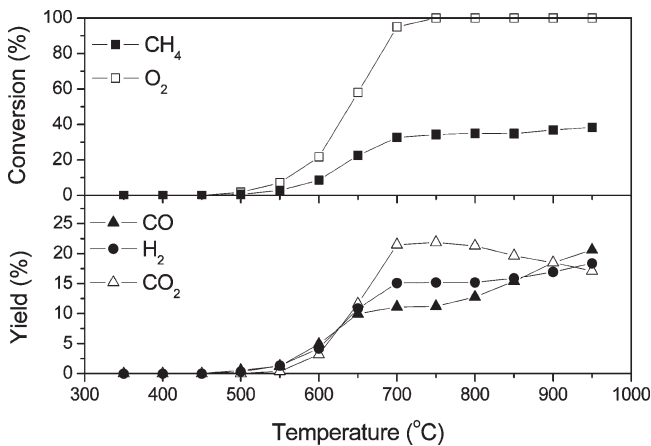


Figure 7. Influence of the reaction temperature on CH_4 oxidation in a fixed-bed reactor over $\text{La}_4\text{Sr}_8\text{Ti}_{12}\text{O}_{38-\delta}$ at an O_2/CH_4 ratio equal to 0.5 ($F_{\text{CH}_4} = 10 \text{ mL min}^{-1}$, $F_{\text{total}} = 100 \text{ mL min}^{-1}$, N_2 balanced).

from 650 to 900°C , selectivity to CO is higher than that to CO_2 at temperatures below 650°C and above 900°C .

It is noticed that the oxidation products of methane strongly depend upon the O_2/CH_4 ratios in the reactants at 950°C , as shown in Figure 8. Full oxidation of CH_4 may be observed in an oxygen-rich atmosphere when the O_2/CH_4

(33) Triantafyllopoulos, N. C.; Neophytides, S. G. *J. Catal.* 2003, 217, 324–333.

(34) Triantafyllopoulos, N. C.; Neophytides, S. G. *J. Catal.* 2006, 239, 187–199.

(35) He, H. P.; Vohs, J. M.; Gorte, R. J. *J. Power Sources* 2005, 144, 135–140.

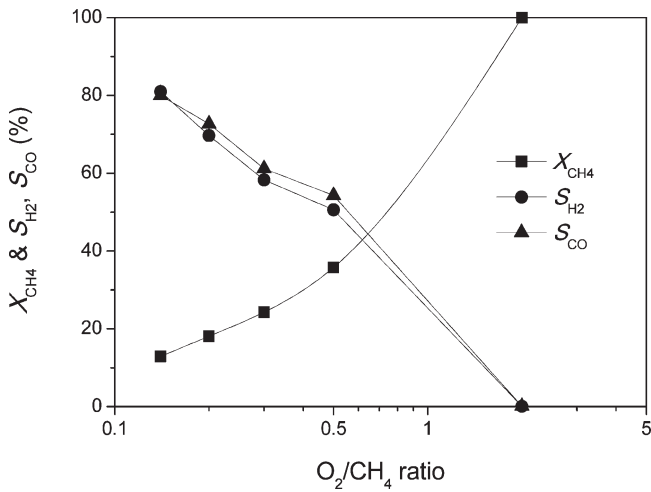


Figure 8. Influence of the O₂/CH₄ ratio on CH₄ oxidation in a fixed-bed reactor over La₄Sr₈Ti₁₂O_{38-δ} at 950 °C ($F_{CH_4} = 10 \text{ mL min}^{-1}$, $F_{total} = 100 \text{ mL min}^{-1}$, N₂ balanced).

ratio is equal to 2 or higher. However, the main products of CH₄ oxidation are syngas in the case of the O₂/CH₄ ratio at 0.5, where approximately 54% CO and 51% H₂ selectivity can be obtained. When the O₂/CH₄ ratio decreases from 0.5 to a further oxygen-lean atmosphere, both CO and H₂ selectivity improve apparently, although the corresponding CH₄ conversion is limited because of the less oxygen available. The highest selectivity to both CO and H₂ around 80% at 13% CH₄ conversion is achieved at the minimum O₂/CH₄ ratio of 0.12 in the present investigation. It is also noted that the ratios of H₂/CO in the products of the POM reaction are almost constant and close to the ideal ratio of syngas at 2.0 within experimental error in all of the cases of oxygen-lean reaction conditions.

The reforming reactions of methane were carried out over the La₄Sr₈Ti₁₂O_{38-δ} catalyst under the given conditions in the presence of CO₂ or H₂O, respectively. In contrast, no obvious CH₄ conversion was detected during the blank reaction using quartz particles, except for a trace of H₂ at temperatures above 950 °C. As shown in Figure 9, the initial reaction temperature for CO₂ reforming of CH₄ is above 800 °C. CH₄ conversion reaches 8.8% at 950 °C, whereas the formation rates of CO and H₂ are equal to 1.59 and 0.41 mL min⁻¹, respectively. Besides the major products CO and H₂, H₂O should also exist in the product as deduced from the mass balance. Figure 10 shows the performance of steam reforming of CH₄ as a function of the reaction temperature. The steam reforming reaction occurs initially at 850 °C and then increases apparently with the temperature. CH₄ conversion reaches 4.9% at 950 °C, whereas an obvious amount of CO and H₂ may be produced with the formation rates of 0.13 and 0.85 mL min⁻¹, respectively. In addition to the major reforming products CO and H₂, CO₂ is also detected in the product mixture at temperatures above 900 °C.

4. Discussion

Partial oxidation of methane to syngas may occur via two generally possible mechanisms.¹ One is a direct partial oxidation mechanism, during which the primary products can be formed by the combination of surface carbon and oxygen species; the other is an indirect mechanism involving full oxidation of methane followed by reforming reactions. The indirect route is characterized by the consumption of all

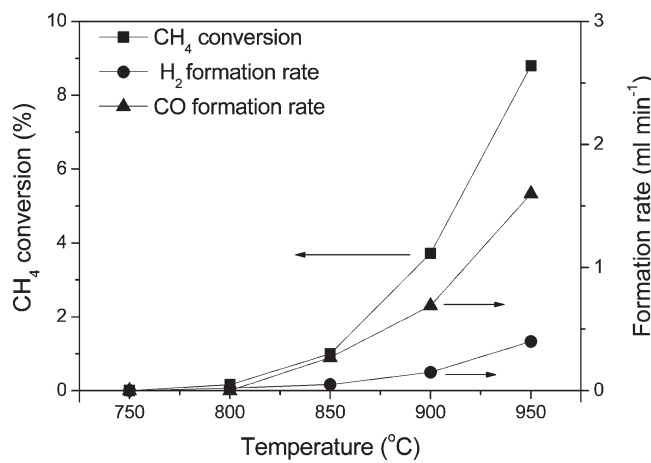


Figure 9. CO₂ reforming of CH₄ over La₄Sr₈Ti₁₂O_{38-δ} at different temperatures (CO₂/CH₄ = 1:1, $F_{CH_4} = 5 \text{ mL min}^{-1}$, $F_{total} = 100 \text{ mL min}^{-1}$, N₂ balanced).

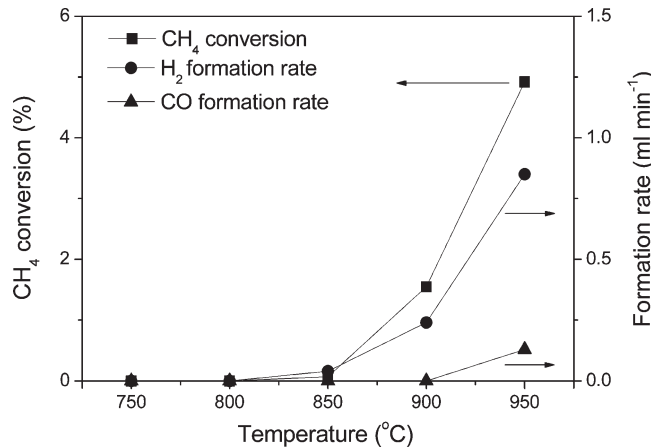


Figure 10. Steam reforming of CH₄ over La₄Sr₈Ti₁₂O_{38-δ} at different temperatures (H₂O/CH₄ = 0.45:1, $F_{CH_4} = 5 \text{ mL min}^{-1}$, $F_{total} = 100 \text{ mL min}^{-1}$, N₂ balanced).

oxygen for methane combustion prior to the significant formation of CO and H₂. Therefore, the direct partial oxidation may be deduced from the facts of the presence of apparent CO and H₂ in the products before both the full conversion of oxygen and the occurrence of CO₂ or steam reforming. From the results of oxidation and reforming of CH₄ in fixed-bed reactor, appreciable yields of syngas can be detected before 750 °C, at which all oxygen is converted (Figure 7). At the same time, both CO₂ and steam reforming of methane may only be possibly initiated after 800 °C (Figures 9 and 10). These facts evidently indicate that the primary products CO and CO₂ are not interconvertible at reaction temperatures less than 800 °C. Moreover, the obvious activities of reforming reactions at rather high temperatures greater than 850 °C give rise to the increasing yields of CO and H₂ at the expense of the CO₂ yield, which suggests that both direct and indirect mechanisms take effect under this condition.

It has been established that lattice oxygen species are active for POM over some mixed oxide catalysts. The lattice oxygen rather than gaseous O₂ has been proven as an oxidant for the production of CO and/or H₂ by means of the CH₄ pulse reaction over YSZ³⁶ and LaFeO₃²² and La_{1-x}Sr_xMnO₃-based

(36) Zhu, J. J.; van Ommen, J. G.; Bouwmeester, H. J. M.; Lefferts, L. *J. Catal.* **2005**, 233, 434–441.

perovskite oxides,²³ temperature-programmed reaction over Gd- and Nb-doped ceria,^{20,21} as well as isotopic oxygen-exchange investigation.³⁶ Oxidation of methane may proceed via a Mars–van Krevelen mechanism, during which lattice oxygen is responsible for methane activation and involved into the final products, followed by replenishment of the extracted lattice oxygen through the dissociative adsorption of molecular oxygen at the surface.^{18,36}

The direct partial oxidation of methane over the oxide catalyst has been proposed to proceed via the decomposition of the surface formaldehyde intermediate, resulting from the activation of methane by surface lattice oxygen species, while CO₂ may be formed by the decomposition of carbonate species, originated from the further oxidation of the surface intermediate.^{18,19} According to these reaction mechanism schemes, the formation of CO requires less surface lattice oxygen species than CO₂ formation and a lower concentration of gas-phase oxygen results in less full oxidation of the desorbed surface formaldehyde intermediate. This would explain the observation in Figure 8 that the decreasing O₂/CH₄ ratio favors the increasing CO and H₂ selectivity for POM in the fixed-bed reactor, because a small O₂/CH₄ ratio corresponds to a low concentration of gas-phase oxygen and the equilibrated surface lattice oxygen species by considering oxygen activation comparatively fast as compared to methane activation.^{18,36}

The activity for POM over La₄Sr₈Ti₁₂O_{38-δ} in the fixed-bed reactor is comparable to the previous results over representative YSZ³⁷ and Ca_{0.8}Sr_{0.2}TiO₃³⁸ catalysts under similar reaction conditions. At 800 °C and an O₂/CH₄ ratio equal to 0.5, oxygen conversion can reach 100% for YSZ³⁷ and La₄Sr₈Ti₁₂O_{38-δ} in the present work, while oxygen conversion can only reach 84.4% for Ca_{0.8}Sr_{0.2}TiO₃,³⁸ besides, higher H₂ selectivity can be obtained for La₄Sr₈Ti₁₂O_{38-δ} than for both YSZ and Ca_{0.8}Sr_{0.2}TiO₃.

It is noteworthy that the activity for POM is much higher in the SDC–LSC membrane reactor than in the fixed-bed reactor, as compared in Table 1. When operating in the membrane reactor at a CH₄ feed rate of 20 mL min⁻¹, the O₂/CH₄ ratio is also equal to 0.2 by taking into account the corresponding oxygen permeation rate of 0.63 mL cm⁻² min⁻¹ and membrane tube surface area of 6.25 cm². At the identical O₂/CH₄ ratio and reaction temperature of 950 °C, methane oxidation in the membrane reactor exhibits greatly enhanced CH₄ conversion as well as selectivity to CO and H₂ in comparison to the reaction in the fixed-bed reactor.

The difference in the reactivity for both reactors may originate from their different manner of supplying oxygen. In the case of the fixed-bed reactor, gaseous oxygen is co-fed with methane and subsequently activated at the catalyst surface into the final lattice oxygen species to take part in the reaction. The concentration of lattice oxygen species equilibrated with the gaseous oxygen may remain relatively high and almost constant for the catalysts in the fixed-bed reactor, because the concentration of free surface O²⁻ sites do not significantly vary with the oxygen partial pressure¹⁸ at a given O₂/CH₄ ratio. With respect to the membrane reactor, the oxygen is supplied in a controlled and distributed way through the membrane tube to the inner side contacting the catalyst

and reactants,⁵ which may alter the relative presence of different types of active oxygen species (e.g., O²⁻, O⁻, and O₂₋) at the membrane surface.³⁹ This process basically involves the oxygen permeation through the membrane and the migration from the membrane to the catalyst surface. The transport of lattice oxygen ions in the bulk of the SDC–LSC membrane is mainly the limited step during the overall process at a given temperature.¹² Considering that an oxygen chemical potential gradient exists during the whole oxygen permeation and migration pathway as the driving force,⁵ it is reasonable to expect a relatively low concentration of lattice oxygen sites for the La₄Sr₈Ti₁₂O_{38-δ} catalyst in the membrane reactor. Additionally, there is hardly gaseous oxygen existing inside the membrane reactor under the applied reaction conditions. This may account for the much higher CO and H₂ selectivity and, thus, enhanced CH₄ conversion in the membrane reactor than in the fixed-bed reactor.

In comparison to nickel metal-based catalysts, La₄Sr₈Ti₁₂O_{38-δ} exhibits favorable stability and simple recovering treatment against carbon deposition at the expense of low activity for the POM reaction. The application of the perovskite oxide catalysts for syngas production may be viable by taking advantages of the proposed concepts of the two-stage oxygen-permeable membrane reactor⁷ with a dual catalyst bed.⁴⁰ The first stage consists of La₄Sr₈Ti₁₂O_{38-δ} packed in the oxygen-permeable membrane for partially selective oxidation of CH₄ by the reaction with oxygen permeated through the membrane. The resultant mixture is consecutively transferred to the second stage of the Ni metal catalyst bed, where the remaining methane is reformed in complete conversion to syngas if an appropriate O₂/CH₄ ratio is controlled. The partially selective oxidation in the first stage can decrease significantly the amount of heat generated in comparison to the initial deep oxidation of a single Ni metal catalyst bed for POM,⁴⁰ which may not only circumvent the catalyst deactivation but also reduce the requirement on the stability of the membrane materials.⁷

The present investigation may also give some clues to the catalytic behavior of La₄Sr₈Ti₁₂O_{38-δ} as a SOFC anode material for the direct methane fuel cell. The oxygen permeation through the SDC–LSC dual-phase composite membrane involves transport of oxygen ions through the SDC phase and countermovement of electrons in the LSC phase,¹² besides the interphase oxygen exchange. In accordance with this transport scheme, the membrane reactor consisting of the oxygen permeation cell in combination with the SOFC anode material can be essentially regarded as an internally short-circuited fuel cell. Thus, the methane oxidation in the membrane reactor may reflect the catalytic properties of SOFC anode materials for the direct methane fuel cell. In comparison to the previous efforts to reveal these catalytic properties by simulating the SOFC anode operating environment in the conventional fixed-bed reactor,^{41–43} our approach employing the membrane reactor may provide better replication of the SOFC anode environment in view of a similar oxygen supply manner, oxygen partial pressure, and reaction atmosphere. Never-

(39) Gellings, P. J.; Bouwmeester, H. J. M. *Catal. Today* **1992**, *12*, 1–105.

(40) Zhu, J.; Rahuman, M.; van Ommen, J. G.; Lefferts, L. *Appl. Catal., A* **2004**, *259*, 95–100.

(41) Tao, S. W.; Irvine, J. T. S. *Chem. Mater.* **2004**, *16*, 4116–4121.

(42) Tao, S. W.; Irvine, J. T. S.; Plint, S. M. *J. Phys. Chem. B* **2006**, *110*, 21771–21776.

(43) van den Bossche, M.; McIntosh, S. J. *Catal.* **2008**, *255*, 313–323.

(37) Zhu, J. J.; van Ommen, J. G.; Knoester, A.; Lefferts, L. *J. Catal.* **2005**, *230*, 291–300.

(38) Hayakawa, T.; Harihara, H.; Andersen, A. G.; Suzuki, K.; Yasuda, H.; Tsunoda, T.; Hamakawa, S.; York, A. P. E.; Yoon, Y. S.; Shimizu, M.; Takehira, K. *Appl. Catal., A* **1997**, *149*, 391–410.

theless, further improvements should be made with respect to the geometry of the membrane reactor and the interconnection manner between the anode and membrane materials. Tao et al. have concluded that the electrochemical performance of the $\text{La}_{0.75}\text{Sr}_{0.25}\text{Cr}_{0.5}\text{Fe}_{0.5}\text{O}_{3-\delta}$ anode is inferior to that of $\text{La}_{0.75}\text{Sr}_{0.25}\text{Cr}_{0.5}\text{Mn}_{0.5}\text{O}_{3-\delta}$, because the complete methane oxidation activity, rather than methane partial oxidation and reforming activities, of the Mn analogue under most conditions can play an important role in the SOFC anode process.^{41,42} Our results suggest that $\text{La}_4\text{Sr}_8\text{Ti}_{12}\text{O}_{38-\delta}$ exhibits appreciable activity for the POM reaction and insufficient activity for complete methane oxidation under the simulated SOFC anode operating environment in the membrane reactor, which is consistent with its moderate electrochemical performance compared to those of the state of the art materials for direct methane use fuel cells.^{30,31}

5. Conclusions

The results of the present study revealed that the perovskite-type oxide $\text{La}_4\text{Sr}_8\text{Ti}_{12}\text{O}_{38-\delta}$, previously applied as potential SOFC anode material for the direct CH_4 fuel cell, can exhibit appreciable activity for the partial oxidation of methane to syngas conducted with the SDC–LSC membrane reactor. The catalytic properties are strongly influenced by both the reaction temperature and CH_4 feed rate or O_2/CH_4 ratio. Under the optimized operating conditions in the membrane

reactor at 950 °C and CH_4 feed rate of 20 mL min⁻¹, the syngas production rate as high as 2.45 mL cm⁻² min⁻¹ with the ideal ratio of H_2/CO (ca. 2.0) can be achieved for approximately 88% CO and 89% H_2 selectivity at 30% CH_4 conversion. A direct partial oxidation mechanism below 800 °C may be deduced from a comparative study with a conventional fixed-bed reactor, while obvious CO_2 and steam reforming reactions occur above 850 °C. The proposed reaction pathway mainly involves lattice oxygen species responsive for methane activation and as an oxidant for the production of syngas via a surface formaldehyde intermediate, which may entail less surface lattice oxygen species for higher selectivity to partial oxidation. This is consistent with the results that the decreasing O_2/CH_4 ratio favors the increasing CO and H_2 selectivity and that the reactivity for POM is greatly enhanced in the membrane reactor than in the fixed-bed reactor because of their different manner of supplying oxygen. The present approach employing a membrane reactor may also provide insight into the catalytic reaction of SOFC anode material for the direct methane fuel cell by a simulating anode operating environment.

Acknowledgment. The authors are grateful for the financial support from the National Natural Science Foundation of China (Grant 20703042) and the China Postdoctoral Science Foundation.